Int. J. Electrochem. Sci., 16 **(2021)** Article ID: 21072, doi: 10.20964/2021.07.48

International Journal of
ELECTROCHEMICAL
SCIENCE
www.electrochemsci.org

Short Communcation

Structural and Photoelectrochemical Studies of CdS Quantum Dots and Its Use as Photocatalyst for Methylene Blue Dye Degradation

Peter A. Ajibade[*] *Athandwe M. Paca and Lebogang L. R. Mphahlele*

School of Chemistry and Physics, University of KwaZulu-Natal, Private Bag X01, Scottsville, Pietermaritzburg, 3209, South Africa
[*]E-mail: ajibadep@ukzn.ac.za

Received: 27 January 2021 / *Accepted:* 15 April 2021 / *Published:* 31 May 2021

We report the influence of capping agents on the structural, photoelectrochemical and photocatalytic degradation of methylene blue (MB) dyes of monodispersed oleylamine (OLM) and octadecylamine (ODA) capped cadmium sulfide (CdS) quantum dots (QDs). Powder X-ray diffraction (pXRD) patterns of the as-prepared CdS QDs confirmed that QDs possess a hexagonal crystalline phase irrespective of the capping agents. TEM micrographs showed monodispersed spherically shaped CdS QDs with particle sizes of 3.16-5.68 and 4.71-5.61 nm for OLM-CdS and ODA-CdS QDs, respectively. The estimated band gap energy from Tauc plots were found to be 2.00 and 2.04 eV for OLM-CdS and ODA-CdS QDs, indicating that the as-prepared CdS QDs are quantum confined due to their small sizes and absorption band edges that are blue-shifted. Electrochemical band gaps were found to be 0.25 mV/s for OLM-CdS and 0.99 mV/s for ODA-CdS. The prepared CdS QDs were then used as photocatalysts for the degradation of MB dye and yielded a degradation efficiency of 65% for OLM-CdS and 76% for ODA-CdS QDs. This confirmed that the capping agent influences the photocatalytic degradation efficiency of the as-prepared CdS quantum dots.

Keywords: CdS, quantum dots, capping agents, photodegradation, methylene blue.

1. INTRODUCTION

Cadmium sulfide (CdS) nanoparticles find application in nonlinear optics, optoelectronic and other electronic devices [1-2]. One of the major method employed for preparing CdS nanoparticles is the thermolysis of metal complexes of dithiocarbamate [3-5], alkyl xanthates [6], *N*-alkyl thiourea [7] in the presence of high boiling point reagents that act as capping agents. Although many semiconductors

are being studied for use as photocatalysts, the energy band gap of CdS which is approximately 2.5eV is of paramount importance because it gives the CdS wide range in the visible region as its size is reduced [8,9]. There are large number of reports on the use of CdS QDs in photocatalysis, solar cells, and electrochemistry [9-11]. It has been reported that CdS nanoparticles as photocatalysts can be useful in environmental remediation and energy applications [11]. Abdolraouf *et al.* [10] reported CdS quantum dots as photocatalysts with percentage degradation of 98%. The electrochemical behaviour of CdS QDs demonstrated the quantized electronic behavior and also the decomposition processes during the redox reactions [12].

The use of CdS nanoparticles as photocatalysts is ascribed to its energy band gap which corresponds with the visible region of the electromagnetic spectrum [13-16] and thus can effectively harness solar energy [17]. As a result, they are explored for wastewater remediation [18]. Although, CdS are not regarded as excellent photocatalyst because small CdS particles can readily aggregate into larger particles, resulting in smaller surface area and enhanced recombination affinity of photogenerated electron-deficiency and therefore limits the photocatalytic efficiency [19,20]. To solve this limitation, numerous procedures have utilized to fabricate CdS nanoparticles [21]. Thermal decomposition of single-source precursors could lead to monodispersed semiconductor CdS nanomaterials [22].

The difficulty of degrading methylene blue under light irradiation makes it a model dye for photocatalytic studies [23,24]. Interest in photocatalysis to remove organic contaminants from contaminated water bodies is because it does not lead to any secondary by products that required special disposal [25,26]. Semiconductors nanocrystals have distinct electron shells and that permit electron movement from the valence band edge ($h1$) to the conduction band edge ($e1$) [27]. Cyclic voltammetry (CV) has been productively utilized for some years to measure the approximation of HOMO-LUMO energy levels of electroactive molecules that are soluble in appropriate solvents [28]. Herein, we report the structural and photoelectrochemical properties of oleylamine (OLM) and octadecylamine (ODA) capped CdS quantum dots and their use as photocatalysts for the degradation of MB dyes.

2. EXPERIMENTAL

2.1 Material and Characterization Techniques

All chemical reagents used in this work were obtained from Merck and used as received. Powder X-ray diffraction (pXRD) scans were recorded by Philips PW1830 X-ray Diffractometer. TEM and HRTEM images were taken by Joel 1400 and Joel HRTEM 2100 electron microscopes. SEM and EDS images were capture by a ZEISS EVO LS 15 microscope. Perkin Elmer LS 45 fluorescence spectrometer was used to record the photoluminescence measurements. FTIR spectra were obtained by a Carry 630 FTIR spectrometer. The ligand and the complex were synthesised using modified procedure given in literature [29,30]. Oleyamine (OLM) and octadecyamine (ODA) capped cadmium sulfide quantum dots were prepared from thermolysis of Cd(II) 4(-2-aminoethyl) morpholinyl dithiocarbamate at 180 °C following literature procedure [31,32].

2.2 Electrochemical evaluation

Electrochemical evaluation was done by a potentiostat/galvanostat instrument. An autolab potentiostat fitted with three-electrodes: a glassy carbon working electrode, Ag/AgCl reference electrode and an auxiliary platinum counter electrode. Dichloromethane (DCM) was used to prepare 2 mM of CdS and 0.1 M of tetrabutylammonium hexafluorophosphate (TBAPF6) solution. The CdS quantum dots solutions were flushed with nitrogen gas for 15 min prior to each run. For each run a sludge of alumina and ultra-pure water on a Buehler felt pad were used to carefully polish the glassy carbon-working electrode [33].

2.3 Degradation of methylene blue dye by CdS quantum dots

Dye solution was prepared and stirred in the dark for 15 min for it to reach equilibrium. CdS quantum dots were then added to the dye solution to catalyze the photocatalytic degradation. The solution with the catalyst was stirred in the dark for 15 min for the solution to attain equilibrium so that the loss of compound due to adsorption can be considered. It was then irradiated with high pressure light and the process was monitored for 3 h. Samples were removed at regular time intervals of 30 min to measure the decrease in concentration of dye. The absorbance and concentration of the samples was examined by a UV-Visible Spectroscopy at the maximum wavelength of the dye. The dye chosen for degradation was methylene blue. The concentration of the dye was 10 ppm [34].

3. RESULTS AND DISCUSSION

3.1 Powder X-ray Diffraction of CdS quantum dots

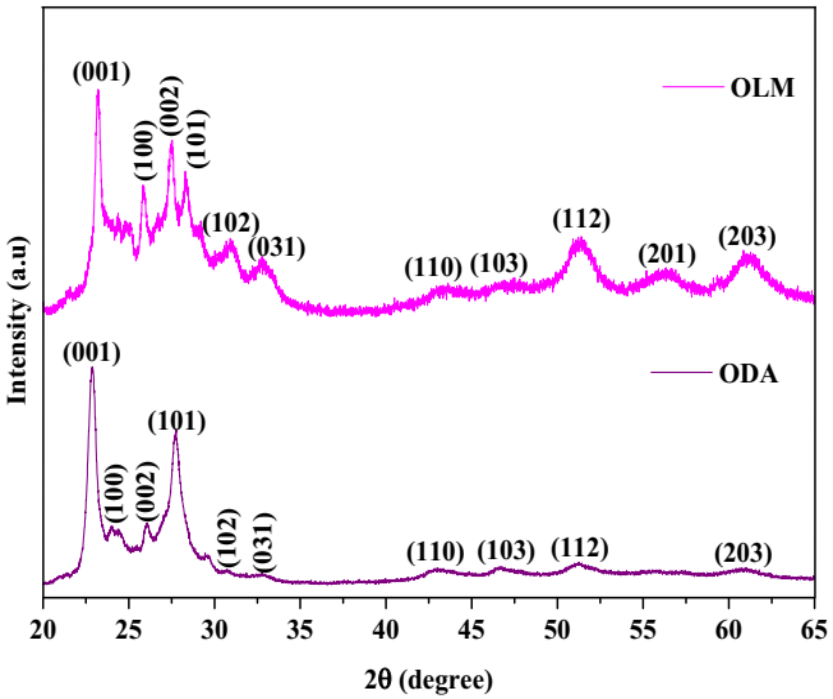

Figure 1. pXRD patterns of CdS QDs with different capping agent at 2θ (degree)

The pXRD patterns of the CdS QDs are shown in Figure 1). The diffraction peaks of OLM-CdS quantum dots were indexed to (100), (100), (002), (101), (102), (031), (110), (103) and (112) planes which corresponded to 23, 27, 28, 31, 33, 34, 51, 56, and 61°, confirming the hexagonal CdS crystalline phases with the ICDD ref code: 00-001-0780 [35-36]. The ODA-CdS quantum dots were indexed to (100), (002), (101), (102), (110), (103), (112), and (203) which corresponded to 23, 26, 28, 33, 43, 47, 51, and 61° of the hexagonal crystalline phases of CdS. There were no impurities detected in the CdS quantum dots. Broad diffraction patterns signify small crystalline size [37].

3.2. Electron microscopic studies

The TEM images of the CdS QDs are shown in Figure 2. TEM image of OLM-CdS QDs showed spherical and semi-spherical shapes, which are uniform and monodispersed.

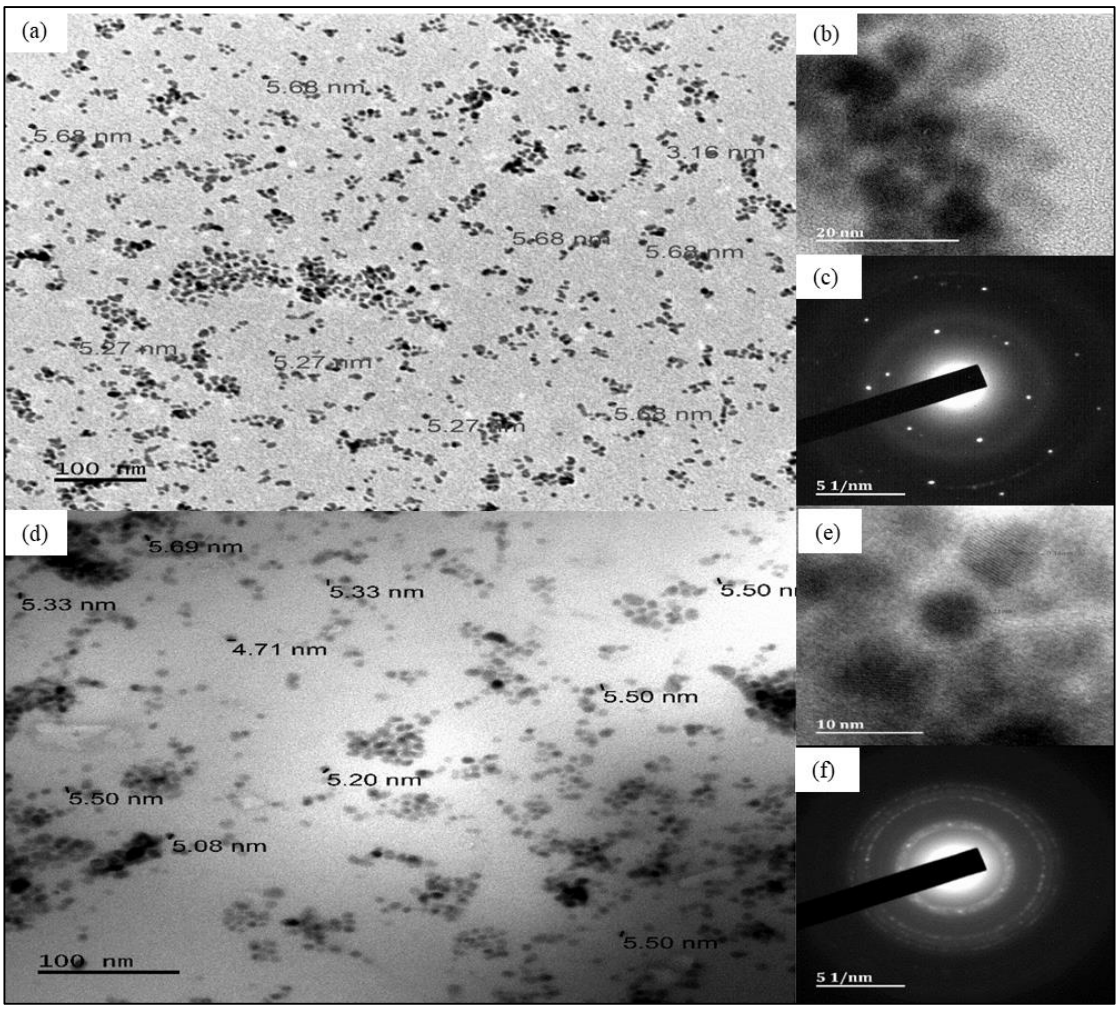

Figure 2. Images of OLM-CdS and ODA-CdS quantums: TEM ((a) and (d)), lattice fringes ((b) and (e)) and SAED ((c) and (f)).

The size of the QDs ranges from 3.16-5.68 nm. The lattice fringes indicated random distribution of the QDs with a spacing distance of 0.34 nm. SAED displayed well-diffracted patterns with small bright spots. TEM image of ODA-CdS QDs showed small spherically shaped particles with some agglomeration and crystallite sizes in the range 4.71-5.69 nm. The lattice fringes revealed that the particles are nano-polycrystalline and unevenly distributed with an interplanar spacing of 0.32 nm. SAED patterns showed that the particles that are not well diffracted, which might be due to agglomeration of the particles. The lattice fringes were blurred with faded contrast, suggesting an excess capping agent on the particles

The surface morphology of the CdS QDs was examined by SEM. SEM image of OLM-CdS QDs showed clustered particles with a freestone smooth surface. These QDs are more on the surface and well distributed. ODA-CdS QDs showed lumpy spherical morphology with a smooth surface and the particles have a uniform size. The surface morphology of the ODA-CdS might be due to the length of the amine group at the end of the chain while the OLM-CdS nanoparticles are affected by the double bond in the middle of the chain which plays the role in capping the particles. EDS confirmed the elements present in the CdS QDs sample.

3.3. FTIR Spectra

FTIR spectra of OLM-CdS and ODA-CdS QDs showed a distinct band around 3306 cm^{-1} which was assigned to the *ν*(N-H) stretching frequency. This reveals that the CdS QDs are stabilized within the capping through the $–NH_2$ group that adsorbed on the surfaces of the QDs. The functional groups present in the precursor are not available which proves that the precursor decomposes during thermolysis, thus no organic moieties are observed on the QDs. Another band observed at about 2905-2851 cm^{-1} was assigned to the *ν*(C-H) of the surfactant (oleic acid) and the capping agents. The other significant band ascribed to the *ν*(C=O) stretching frequency of the –COOH group of the oleic acid was observed at 1634 cm^{-1}.

3.4. Optical studies

The absorption spectra of the CdS quantum dots shows sharp band edges between 300 and 500 nm with a distinct peak maximum around 250 nm for both OLM-CdS and ODA-CdS QDs. This maximum relates to the first optically certified transition sandwiched between the electron hole which is indicative of the monodispersive nature of the compounds [38]. The optical band gaps of the as-prepared quantum dots were determined using the Tauc plots [39], which were found to be 1.99 2.05 eV for OLM-CdS and ODA-CdS QDs, respectively. These band gap energies were blue-shifted with the range of 0.33-0.42 eV with respect to their the bulk CdS (2.41 eV) [40-41]. The blue shift energy of QDs dependents on the crystallite site, the smaller the crystallite the higher the blue shift [42]. The emission measurements of the as prepared CdS QDs were conducted at an excitation wavelength of 480 nm. The emission spectra displayed maxima at 486.6 nm for OLM-CdS and 298.2 nm for ODA-CdS QDs. The high intensity of the emission band-edges signifies that the quantum dots have high crystallinity and are

monodispersed [43]. OLM-CdS QDs emission was found to be higher and broader compared the ODA-CdS QDs and that shows that the capping agent has an effect in the formation of the QDs. The emission maxima were red-shifted in comparison to the absorption band edges [44]. The broad band between 550 and 750 was due to the reincorporation of the confined electron holes in some surface defects of the QDs.

3.5. Photocatalytic studies

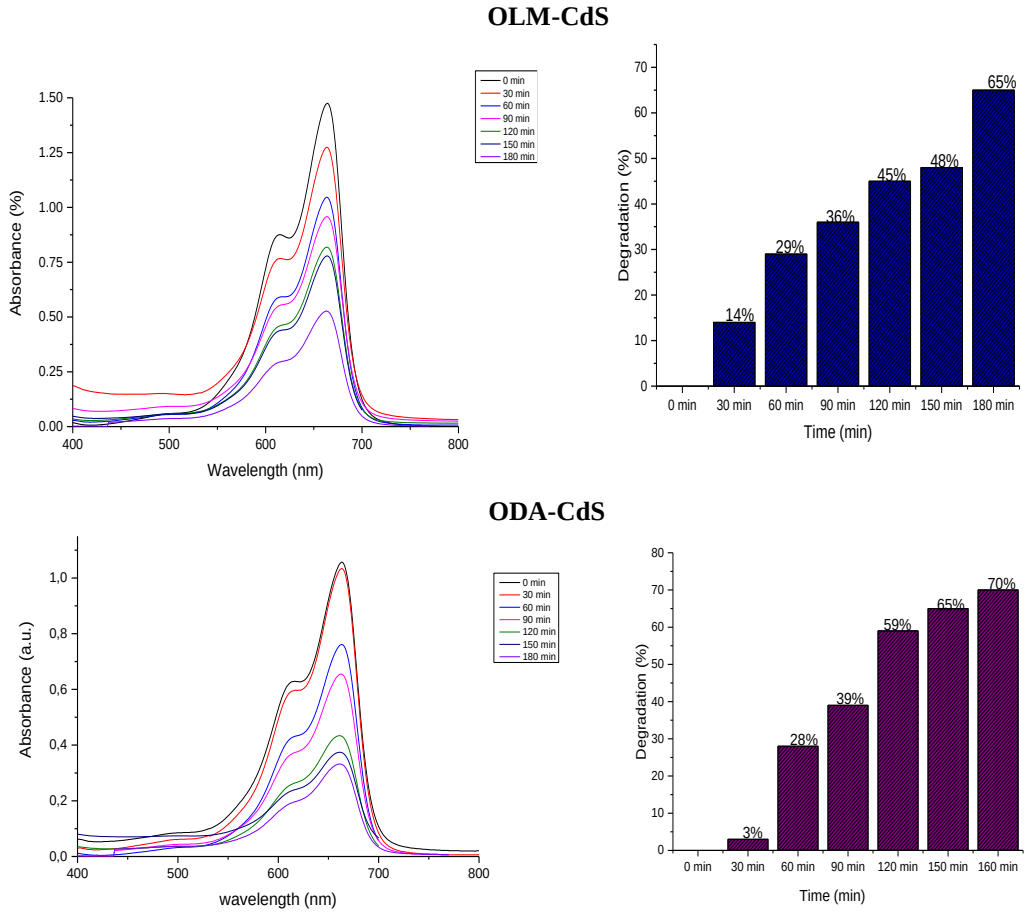

Figure 3. Absorption spectral changes and photodegradation of aqueous MB solution by OLM-CdS and ODA-CdS quantum dots under visible light.

Photocatalyic degradation of methlene blue (MB) dye under mercury lamp irradiation was studied using as-prepared CdS quantum dots catalysts [45]. Figure 3 shows the absorption spectral variations and degradation of aqueous MB dye by CdS QDs. Maximum absorbance of MB was observed at 650 nm. It was observed that the intensity of the absorption bands decreases with increasing exposure. Photocatalystic activity of CdS quantum dots was established by the number of electron-hole pairs on the surface of the photocatalyst. The size of the QDs determines the electron-hole pair recombination owing to the distance of the electron-hole pairs to the electron-hole recombinations. Thus the distance of QDs is short, and it helps the electron-holes to migrate to the surface of the photocatalyst without recoupling. Photocatalytic degradation efficiencies of MB by the OLM-CdS and ODA-CdS were calculated to be 65%, and 70%, respectively, which are knowingly higher than that of bulk-CdS (12.7%)

[46]. Thus ODA-CdS showed the best photocatalytic activity at 3 h. We can conclude from the results that the as-prepared CdS quantum dots are good photocatalyst for degradation of organic pollutants such as dyes under light irradiation. Photodegradation of MB with respect to time in the presence of CdS DQs revealed that the QDs are effective photocatalyst towards methylene dye decolorization. Photo-decomposition efficiency is due to the source of light absorbed by catalyst [47].

3.6. Electrochemical studies

Cyclic voltammetry (CV) was obtained with glass electrode to determine the band gap between HOMO-LUMO of the as-prepared CdS quantum dots to validate Brus model.

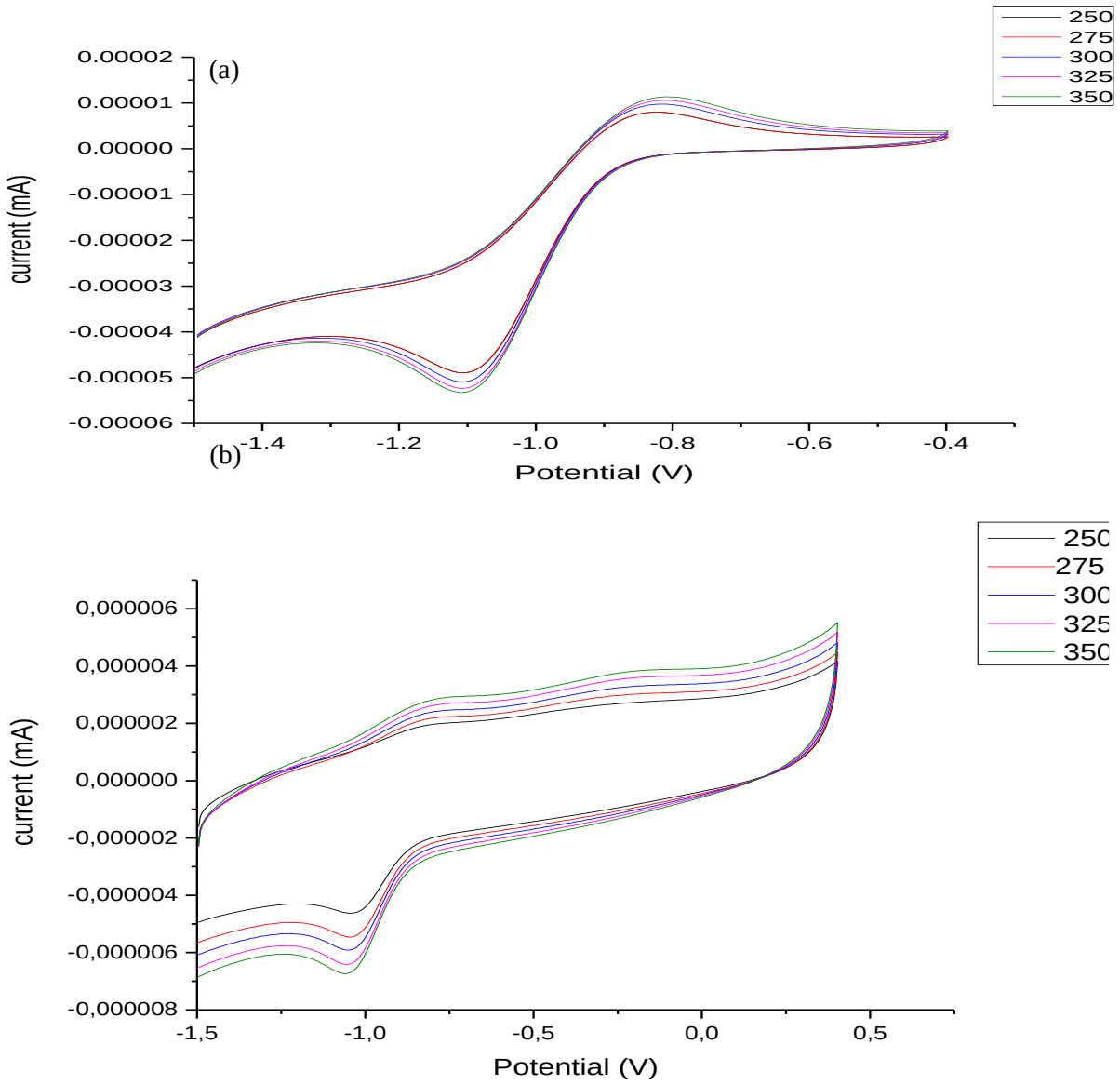

Figure 4. Cyclic voltammetry of OLM-CdS and ODA-CdS quantum dots.

Electrochemical measurement of CdS QDs carried out using cyclic voltammetry (CV) shows clear oxidation-reduction peaks at different regions depending on the CdS quantum dots used. CV was obtained with glass electrode to determine the band gap between HOMO-LUMO to validate Brus model. Extra peaks only emerge on scan reversal after changing either from oxidation to reduction as shown in Figure 4. These peaks are due to diffusion of solution of CdS QDs to the electrode resulting in response to the redox reactions. Thus, the band gap was found to be comparable to those that were obtained from the absorption studies but slightly lower. The correlation of optical and electrochemical band gaps is presented in Table 1. This shows as the size of the as-prepared CdS QDs increase, the energy band gaps increase. Furthermore, indicating that there is charge transfer to the CdS QDs that lead to the consumption of electrons by fast coupled chemical reaction due to the breakdown of the cluster.

Table 1. Relationship between optical and electrochemical band gaps for fractions 250-350 mV/s scan rate

Compounds	250 mV/s –350 mV/S	band gap (eV)	Size (nm)
OLM-CdS	0.25	1.99	5.68
ODA-CdS	0.99	2.05	5.69

4. CONCLUSIONS

Cd(II) 4-(2-aminoethyl) morpholine dithiocarbamate complex was thermolyzed 180°C to prepare OLM and ODA capped CdS quantum dots. The pXRD patterns showed that the both the OLM-CdS and ODA-CdS QDs possess hexagonal crystalline phases. TEM images exhibited partial-spherical monodispersed quantum dots with crystalline sizes ranging between 3.16-5.68 for OLM-CdS and 4.71-5.69 nm for ODA-CdS QDs. The lattice fringes revealed that the particles are very close to each other with interplanar spacing of 0.3 nm for OLM-CdS and 0.34 nm for ODA-CdS QDs. Optical band gaps were found to be 1.99 eV for OLM-CdS and 2.05 eV for ODA-CdS QDs. These band gap energies were found to be blue-shifted with the range of 0.33-0.42 eV compared to the bulk CdS form, which indicate that the as-prepared CdS QDs are quantum confined due to the small particle sizes of the particles. Electrochemical band gaps were found to be 0.25 mV/s for OLM-CdS and 0.99 mV/S for ODA-CdS QDs. Optical band gaps are comparable to the values obtained from the Tauc plots. The percentage degradation of MB dye by the as-prepared CdS quantum dots was 65% and 70% for OLM-CdS and ODA-CdS quantum dots, respectively.

ACKNOWLEDGEMENTS
Financial support of NRF is acknowledged.

References

1. M. Taguchi, I. Yagi, M. Nakagawa, T. Iyoda, Y. Einaga, *J. Am. Chem. Soc.* 128, (2006) 10978.
2. M. Afzaal, Malik, M.A. P. O'Brien, *J. Mater. Chem*. 20, (2010) 4031.
3. A.L. Abdelhady, M. Afzaal, M.A. Malik, P. O'Brien, *J. Mater. Chem.* 21, (2011) 18768.
4. J. Z. Mbese, Peter A. Ajibade *J. Sulf. Chem*., 35 (2014) 438-449.
5. P. A. Ajibade, J. Z. Mbese, B. Omondi, *Synth. React. Met.-Org. Inorg. Nano- Met Chem.* 47 (2017) 202-212.
6. P. A. Ajibade, A. E. Oluwalana, *J. Coord. Chem*. 72 (2019) 3575-3588.
7. J. Osuntokun, P. A. Ajibade, *J. Nanomater.*, 3296071 (2016) 1-14.
8. W. Chengyu, S. Huamei, T. Ying, Y. Tongsuo, Z. Guowu, *Sep. Purif. Technol.* 32, (2003) 357.
9. A. Samadi-Maybodi, M.-R. Sadeghi-Maleki, *Spectrochim. Acta Part A*, 152, (2016) 156.
10. A. Samadi-maybodi, F. Abbasi, R. Akhoondi, *Colloids Surf.* A, 447, (2014) 111.
11. L. Cheng, Q. Xiang, Y. Liao, H. Zhang, *Ener. Environ. Sci.* 11, (2018) 1362.
12. H. Huang, J.-J. Zhu, *Analyst,* 138, (2013) 5855.
13. S.B. Kalia, R. Puri, A. Thakur, J. Christopher, *J. Therm. Anal. Calorim.* 119, (2015) 1619.
14. N. Soltani; E. Saion; W. M. M. Yunus; M. Navasery; G. Bahmanrokh; M. Erfani; M. R. Zare; E. Gharibshahi, *Sol. Energy,* 97 (2013) 147.
15. E. E. El-Katori; M. Ahmed; A. El-Bindary; A. M. Oraby, *J. Photochem. Photobiol*., 392 (2020) 1.
16. R. Rajendran; K. Varadharajan; V. Jayaraman; B. Singaram; J. Jeyaram, *Appl. Nanosci*.,8 (2018) 61.
17. J. Yan; K. Wang; H. Xu; J. Qian; W. Liu; X. Yang; H. Li, *Chinese J. Catal.*, 34 (2013) 1876-1882.
18. M. Nagamine; M. Osial; K. Jackowska; P. Krysinski; J. Widera-Kalinowska, *J. Mar. Sci. Eng.,* 8 (2020) 1.
19. R. Rajendran; V. Jayaraman; K. Varadharajan, J. Phys. Chem. Solids, 129 (2019) 261-269.
20. A. Malathi; J. Madhavan *J. Nano Res.*, 48 (2017) 49.
21. W. Hussain; H. Malik; A. Bahadur; R. Hussain; M. Shoaib; S. Iqbal; H. Hussain; I. Green; A. Badshah; H. Li, *Kinet. Catal.* 59 (2018) 710.
22. I. Jen-La Plante; T. W. Zeid; P. Yang; T. Mokari, *J. Mater. Chem.*, 20 (2010) 6612-6617.
23. S. Balu; K. Uma; G.-T. Pan; T. Yang; S. Ramaraj, *Materials*, 11 (2018) 1030.
24. R. S. Ganesh; E. Durgadevi; M. Navaneethan; S. K. Sharma; H. Binitha; S. Ponnusamy; C. Muthamizhchelvan; Y. Hayakawa, *Chem. Phys. Lett.,* 684 (2017) 126.
25. D. Beydoun; R. Amal; G. Low; S. McEvoy, *J. Nanopart. Res.*, 1 (1999) 439.
26. A. Kumar; G. Pandey, *Mater. Sci. Eng. Int. J,* 1 (2017) 106-114.
27. S. N. Inamdar; P. P. Ingole; S. K. Haram, *ChemPhysChem,* 9 (2008) 2574.
28. A. Ayadi; A. Szukalski; A. El-Ghayoury; K. Haupa; N. Zouari; J. Myśliwiec; F. Kajzar; B. Kulyk; B. Sahraoui, *Dyes Pigm.*, 138 (2017) 255.
29. L. L. Mphahlele; P. A. Ajibade, *J. Sulfur Chem.*, (2019) 648.
30. F.P. Andrew, P.A. Ajibade, *J. Coord. Chem*. 16-18, (2018) 2776
31. A. M. Paca, P. A. Ajibade (2017). *Mater. Chem. Phys*. 202, 143-150.
32. N. L. Botha, P. A. Ajibade, *Mater. Sci. Semicond. Process*. 43, (2016). 149-154.
33. P.A. Ajibade, F.P Andrew, NL Botha, N Solomane, *Molecules* 25 (2020) 3584.
34. P.A. Ajibade, L.R. Mphahlele, *J. Nano Res.* 66, (2021) 103-111.
35. A. Khataee, A. Movafeghi, F. Nazari, F. Vafaei, M.R. Dadpour, Y. Hanifehpour, S.W.T. Joo, *J. Nanopart. Res.* 16, (2014) 2774.
36. N. Shanmugam, B. Saravanan, R. Reagan, N. Kannadasan, K. Sathishkumar, S. Cholan, *Mod. Chem. Appl*. 2, (2014) 124.
37. A. Sabah, S.A. Siddiqi, S. Ali, *World Acad. Sci. Engineer. Technol.* 69, (2010) 82.

38. P. Yan, Y. Xie, Y. Qian, X. Liu, *Chem. Commu.* 14, (1999) 1293.
39. D. Patidar, K. Rathore, N. Saxena, K. Sharma, T. Sharma, *J. Nano. Res*. 97, (2008)
40. P. Bindu, S. Thomas, *Acta Phys. Pol. A,* 131, (2017) 1474.
41. L. Spanhel, M. Haase, H. Weller, A. Henglein, *J. Am. Chem. Soc*. 109, (1987) 5649.
42. W.W. Yu, L. Qu, W. Guo, X. Peng, *Chem. Mater.* 15, (2003) 2854.
43. G. Shen, J.H. Cho, J.K. Yoo, G.-C. Yi, C.J. Lee, *J. Phys. Chem*. B, 109, (2005) 9294.
44. S. Kiprotich, M.O. Onani, F.B. Dejene, *J. Mater. Sci. - Mater. Electron.* 29, (2018) 6004.
45. R.F. Kadhim, *Iraqi J. Phys* 15, (2017) 11.
46. N. Soltani, E. Saion, M.Z. Hussein, M. Erfani, A. Abedini, G. Bahmanrokh, M. Navasery, P. Vaziri, *Int. J. Mol. Sci*. 13, (2012) 12242.
47. T. Senasu, S. Nanan, *J. Mater. Sci.-Mater. Electron.* 28, (2017) 1742.